International Journal of Impact Engineering 180 (2023) 104725

Contents lists available at ScienceDirect

International Journal of Impact Engineering

journal homepage: www.elsevier.com/locate/ijimpeng

Realization of shorter substitutes for a percussive rock drill hammer by periodic redistribution of its mass and compliance

J. Huo [a], B. Lundberg [b,*]

[a] Sandvik Mining and Rock Technology, Sandviken SE-811 81, Sweden
[b] The Ångström Laboratory, Uppsala University, Box 35, Uppsala SE-751 03, Sweden

ARTICLE INFO

Keywords:
Percussive rock drill
Hammer
Substitute
Characteristic impedance
Impact force
Efficiency

ABSTRACT

In percussive drilling of rock, use is made of high-amplitude short-duration force pulses generated through impacts of a hammer on a drill bit or a drill rod assembly. The mass of the hammer is crucial for the impact velocity and the impact frequency, while its length and variation of characteristic impedance control the duration and shape of the force pulses. High efficiency of conversion of kinetic impact energy to work results if the force pulses have suitable shapes and durations. Commonly, hammers of hydraulic rock drills are nearly uniform and generate nearly rectangular force pulses admitting high efficiencies. When space is constrained, short hammers are advantageous as they allow short rock drills. Here, therefore, shorter substitutes for uniform original hammers are sought. They should have the same mass as the original hammer, be shorter than the original hammer, and generate approximately the same impact force history as the original hammer. A method based on 1D theory is developed for realization of substitute hammers with axially periodic characteristic impedance. Impact force histories generated by such hammers agree well with that generated by a uniform original hammer in a 1D context, and also in a 3D context if 3D effects are small enough. Also, for bit-rock interaction conditions from soft to hard, the efficiencies obtained by use of substitute hammers agree well with that obtained by use of the original hammer.

1. Introduction

In percussive drilling of rock, use is made of high-amplitude short-duration force pulses and waves generated through impacts of a hammer on a drill bit like in down-the-hole drilling, or on a drill rod assembly like in top hammer drilling. Between impacts, the hammer is accelerated to its impact velocity by forces with relatively low amplitude and long duration, commonly generated by hydraulic pressure. For given such forces, the mass of the hammer controls the impact velocity and the impact frequency, while the length of the hammer and its distribution of mass and compliance control the duration and shape of the force pulses and waves generated through impact.

High efficiency of conversion of kinetic impact energy to work associated with rock crushing results if the impact-generated force pulses and the related waves in the rock drill have shapes and durations that depend on the type of drilling process, the number, distribution and geometry of hard-metal buttons under the drill bit, and the properties of the rock [1–5]. Ideally, these force pulses and waves should have amplitudes that increase with the force required for continued penetration. Then they should abruptly drop to zero. In general, however, hammers producing such force pulses through axial impact cannot be realized [6,7].

Commonly, hydraulic rock drill hammers are nearly uniform and generate force pulses and waves of nearly rectangular shape. Use of such hammers, shorter in hard rock and longer in soft rock, results in efficiencies as high as 70–80 percent [4,5].

In underground applications with space constraints, short rock drills may be advantageous. For a uniform original hammer, therefore, it is of interest to explore the existence of substitute hammers that are shorter, have the same mass, and produce approximately the same rectangular force pulse as the original hammer. Replacement of the original hammer with such a shorter substitute hammer would allow a shorter rock drill with the same performance (impact energy, impact frequency and efficiency) as the original drill.

In direct problems of longitudinal impact, the axial variation of characteristic impedance of the impacting bodies and the impact velocity are prescribed, and the impact force history is sought. Such problems normally have complete solutions. Examples are given in text books [8] and research papers. Some examples related to percussive

* Corresponding author.
E-mail address: bengt.lundberg@angstrom.uu.se (B. Lundberg).

https://doi.org/10.1016/j.ijimpeng.2023.104725
Received 5 April 2023; Accepted 9 July 2023
Available online 10 July 2023
0734-743X/© 2023 The Authors. Published by Elsevier Ltd. This is an open access article under the CC BY license (http://creativecommons.org/licenses/by/4.0/).

Nomenclature

Latin

A	cross-sectional area
C	compliance of segment
c	elastic wave speed
E	Young's modulus
F	impact force
k	penetration resistance (force per unit penetration)
L	length of hammer ($= nl$)
l	length of segment (($= L/n$)
M	mass of segment
n	number of segments or periods
p	constant ($= 1/2\phi(\theta^{-1} - \theta)$)
t	transit time
V	impact velocity
Z	characteristic impedances

Greek

β	dimensionless penetration resistance
γ	fraction of reversible penetration or work during primary loading
ζ	dimensionless characteristic impedance
η	efficiency of impact energy conversion to work
θ	characteristic-impedance ratio ($= Z_2/Z_0$)
ρ	density of segment
τ	dimensionless transit times
ϕ	length ratio ($= \tau_2/\tau_1$)

Subscripts

0	original hammer
1	middle part of substitute hammer period
2	end parts of substitute hammer period
*	substitute hammer

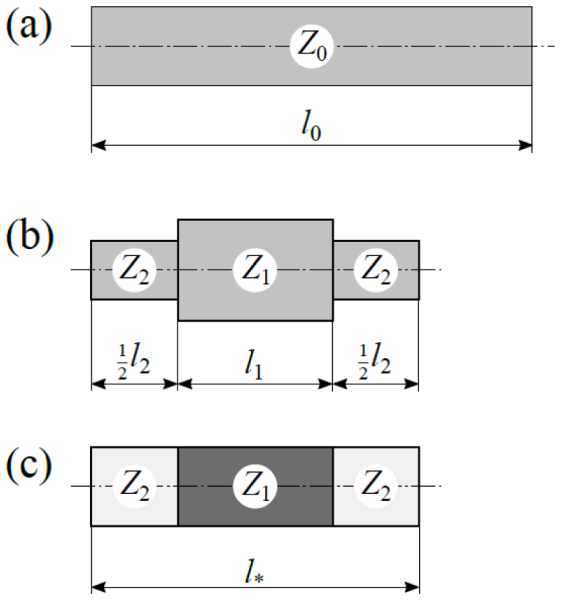

Fig. 1. (a) Uniform segment of original hammer, (b) symmetric period of substitute hammer with constant material and variable diameter, and (c) symmetric period of substitute hammer with constant diameter and variable material.

Table 1
Parameters defining periods of substitute hammers.

Case	ϕ	θ
1a	0.2	0.5
1b	0.2	2.0
2a	1.0	0.5
2b	1.0	2.0

drilling were presented by Dutta [9] and by Luciano & Dante [10]. In inverse problems of longitudinal impact, the impact force history and the impact velocity are prescribed, and the axial variation of characteristic impedance is sought. Such problems have complete solutions only in special cases [11,12]. Recently, Burgert [13] and Burgert et al. [14] developed an algorithm by which inverse problems of longitudinal impact can be solved from initial contact up to a time beyond which the prescribed impact force history cannot be realized by use of non-negative characteristic impedances. In cases where a finite such time does not exist, the algorithm produces the complete solution of the inverse problem.

Table 2
Characteristic impedances, travelling times and hammer length ratios for substitute hammers with $n = 5$, 10 and 20 for 1D simulations.

Case	ζ_1	ζ_2	τ_1	τ_2	L_*/L_0
1a	1.1612	0.5	0.7929	0.1586	0.9515
1b	0.8612	2.0	0.7929	0.1586	0.9515
2a	2.0000	0.5	0.4000	0.4000	0.8000
2b	0.5000	2.0	0.4000	0.4000	0.8000

Table 3
Diameters, lengths, and hammer length ratios for substitute hammers with $n = 5$, 10 and 20 for 3D simulations with constant material and variable diameter.

Case	D_1 [mm]	D_2 [mm]	l_1 [mm]	l_2 [mm]	L_*/L_0
1a	32.3	21.2	63.4	12.7	0.9515
1b	27.8	42.4	63.4	12.7	0.9515
2a	42.4	21.2	32.0	32.0	0.8000
2b	21.2	42.4	32.0	32.0	0.8000

In this paper, a uniform original hammer will be given, and substitute hammers with the following properties will be sought: They should have the same mass as the original hammer, be shorter than the original hammer, and generate approximately the same impact force history as the original hammer (impact velocity and impacted body being the same in the two cases). Thus, while the impact force history is prescribed explicitly in a standard inverse problem of longitudinal impact, it is prescribed implicitly in the problem considered here. The problem considered is also related to the inverse problem of identifying elastic junctions between uniform rods with the same transmission properties as a given junction [15,16].

The paper is organized as follows. In Section 2, a method based on 1D stress wave theory is developed for realization of substitute hammers with axially periodic characteristic impedance. In Section 3, 1D and 3D FE simulations are carried out for substitutes for a uniform original hammer. Axial variation of characteristic impedance is realized primarily by variation of diameter for constant material but for the sake of comparison also by variation of Young's modulus and density for constant diameter. In 1D simulations there is no difference between these cases, but in 3D simulations there is. In this section, also, the efficiencies of kinetic impact energy conversion to work associated with rock

Table 4
Material properties, lengths and hammer length ratios for substitute hammers with $n = 5$, 10 and 20 for 3D simulations with constant diameter and variable material.

Case	E_1 [GPa]	ρ_1 [kg/m^3]	E_2 [GPa]	ρ_2 [kg/m^3]	ν	l_1 [mm]	l_2 [mm]	L_*/L_0
1a	232	9290	100	4000	0.3	63.4	12.7	0.9515
1b	172	6890	400	16,000	0.3	63.4	12.7	0.9515
2a	400	16,000	100	4000	0.3	32.0	32.0	0.8000
2b	100	4000	400	16,000	0.3	32.0	32.0	0.8000

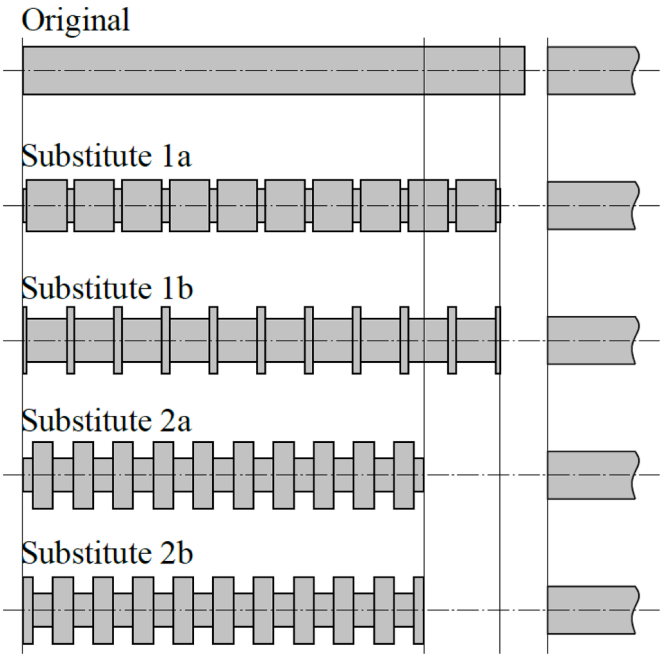

Fig. 2. Uniform original hammer and two pairs of substitute hammers impacting a semi-infinite uniform rod with the same characteristic impedance as the original hammer. The hammers and the rod are made of the same material.

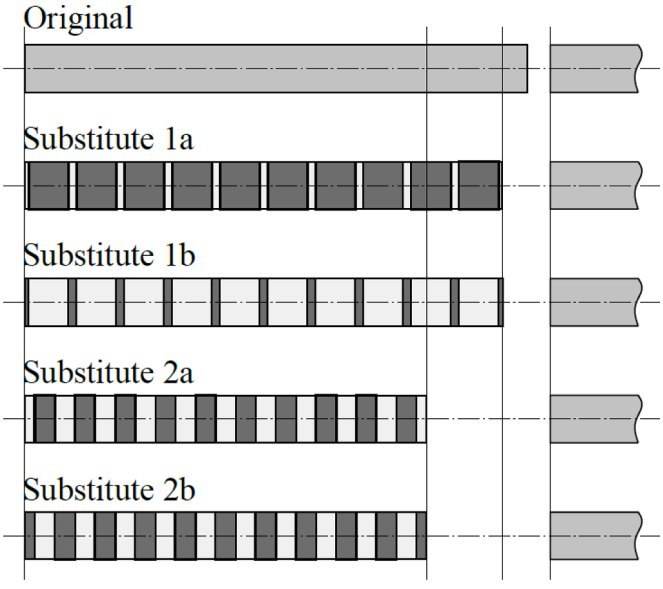

Fig. 3. Uniform original hammer and two pairs of substitute hammers impacting a semi-infinite uniform rod with the same characteristic impedance as the original hammer. The hammers and the rod have the same diameter.

crushing are compared for original and substitute hammers. In Section 4, the results are interpreted and discussed, and in Section 5, finally, main conclusions are summarized.

2. Method

2.1. Original and substitute hammers

The original hammer is assumed to be uniform and have length L_0. It is considered to consist of n identical segments with length $l_0 = L_0/n$, transit time $t_0 = l_0/c_0$, and constant characteristic impedance $Z_0 = A_0(E_0\rho_0)^{1/2}$, where A_0 is the cross-sectional area, E_0 is the Young's modulus, ρ_0 is the density, and $c_0 = (E_0/\rho_0)^{1/2}$ is the elastic wave speed. Such a segment is shown in Fig. 1(a).

A substitute hammer with length L_* and axially periodic characteristic impedance is sought. It is assumed to consist of n equal and symmetric segments of length $l_* = L_*/n$ defined by the transit times $t_1 = l_1/c_1$, $t_2 = l_2/c_2$ and by the characteristic impedances $Z_1 = A_1\ (E_1\rho_1)^{1/2}$ and $Z_2 = A_2\ (E_2\rho_2)^{1/2}$, where l_1 and l_2 are lengths, A_1 and A_2 are cross-sectional areas, and $c_1 = (E_1/\rho_1)^{1/2}$ and $c_2 = (E_2/\rho_2)^{1/2}$ are wave speeds. Such a symmetric hammer period is shown in Fig. 1(b) where the material is constant and in Fig. 1(c) where the diameter is constant.

Each segment of the original hammer has mass $M_0 = Z_0t_0$ and compliance $C_0 = t_0/Z_0$, and each segment of the substitute hammer has mass $M_* = Z_1t_1 + Z_2t_2$ and compliance $C_* = t_1/Z_1 + t_2/Z_2$. Accordingly, the characteristic impedance and the transit time of an original hammer segment can be expressed as $Z_0 = (M_0/C_0)^{1/2}$ and $t_0 = (M_0C_0)^{1/2}$, respectively. The corresponding quantities for a substitute hammer $Z_* = (M_*/C_*)^{1/2}$ and $t_* = (M_*C_*)^{1/2}$, respectively, do not have the same straight interpretations.

2.2. Realization of substitute hammers

The quantities Z_1, Z_2, t_1 and t_2 defining a substitute hammer period are to be expressed in terms of the quantities Z_0 and t_0 defining an original hammer segment so that, if possible, a substitute hammer gets the following properties:

(a) It has the same mass as the original hammer.
(b) For $Z_1 \neq Z_2$ it is shorter than the original hammer.
(c) It generates approximately the same impact force history as the original hammer (impact velocity and impacted body being the same).

The quantities Z_0 and Z_* are crucial for the amplitude of the impact force, while t_0, t_* and n are crucial for its temporal history. If, e.g., the original hammer impacts a rod with the same constant characteristic impedance Z_0 as the hammer, the impact force becomes a rectangular pulse with amplitude $(1/2)Z_0V_0$ and width $2nt_0$, where V_0 is the impact velocity. This choice of original hammer will be made below for numerical simulations.

The quantities (Z_0, t_0) and (Z_*, t_*) are expected to be related similarly to the impact force histories generated by the original hammer and the substitute hammer, respectively. Therefore, it is assumed here that the condition (c) can be fulfilled by choosing $Z_* = Z_0$ and $t_* = t_0$. This *ansatz* is equivalent to $M_* = M_0$ and $C_* = C_0$ which results in the system

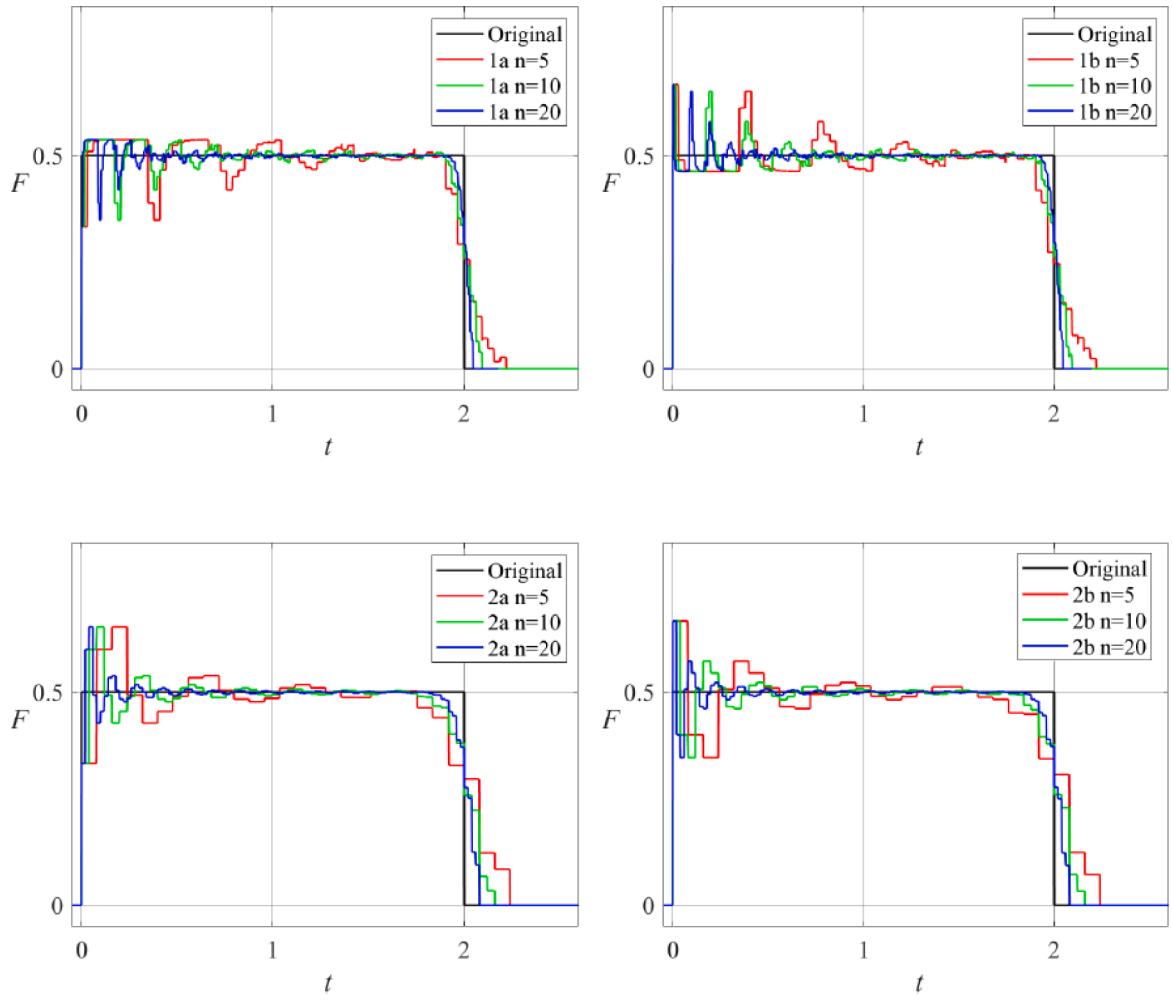

Fig. 4. Impact force histories from 1D simulations of original hammer and substitute hammers impacting a semi-infinite uniform rod with the same characteristic impedance as the original hammer. The substitute hammers are constituted by $n = 5$, 10 and 20 periods, and there is no difference between the cases of constant material and constant diameter.

of two algebraic equations

$$Z_1 t_1 + Z_2 t_2 = Z_0 t_0, \tag{1}$$

$$\frac{t_1}{Z_1} + \frac{t_2}{Z_2} = \frac{t_0}{Z_0} \tag{2}$$

for the four unknown quantities Z_1, Z_2, t_1 and t_2 in terms of the two given quantities Z_0 and t_0. From the first of these equations it follows that the condition a) is satisfied, i.e., the substitute hammer has the same mass as the original hammer. In order for the solution to be unique, two additional relations involving the unknowns are necessary.

The length of the substitute hammer is $L_* = n(c_1 t_1 + c_2 t_2)$ and that of the original hammer is $L_0 = n c_0 t_0$ which gives the hammer length ratio

$$\frac{L_*}{L_0} = \frac{c_1 t_1 + c_2 t_2}{c_0 t_0}. \tag{3}$$

By use of the relations $t_0 = t_* = (M_* C_*)^{1/2}$, the square of this ratio can be expressed as

$$\left(\frac{L_*}{L_0}\right)^2 = \left[(c_1 t_1)^2 + 2 c_1 c_2 t_1 t_2 + (c_2 t_2)^2\right] \Big/ (c_0)^2 \left[t_1^2 + \left(\frac{Z_1}{Z_2} + \frac{Z_2}{Z_1}\right) t_1 t_2 + t_2^2\right]. \tag{4}$$

If the wave speed in the original hammer and those in the substitute hammer are the same, $c_1 = c_2 = c_0$, this result is simplified to

$$\left(\frac{L_*}{L_0}\right)^2 = \left[t_1^2 + 2 t_1 t_2 + t_2^2\right] \Big/ \left[t_1^2 + \left(\frac{Z_1}{Z_2} + \frac{Z_2}{Z_1}\right) t_1 t_2 + t_2^2\right], \tag{5}$$

from which it follows that $L_*/L_0 < 1$ if $Z_1 \neq Z_2$. Thus, if $c_1 = c_2 = c_0$ and $Z_1 \neq Z_2$, the condition b) is fulfilled. In what follows, this will be assumed to be the case.

The extent to which the condition c) is fulfilled, and the relevance of the *ansatz* $Z_* = Z_0$ and $t_* = t_0$, will be demonstrated in cases of impact that will be simulated numerically by use of 1D and 3D models, respectively.

2.3. Results for substitute hammers

With the introduction of dimensionless characteristic impedances $\zeta_i = Z_i/Z_0$ and times $\tau_i = t_i/t_0$, Eqs. (1) and (2) become

$$\zeta_1 \tau_1 + \zeta_2 \tau_2 = 1 \tag{6}$$

$$\frac{\tau_1}{\zeta_1} + \frac{\tau_2}{\zeta_2} = 1, \tag{7}$$

respectively. It is noted that if these equations are satisfied by (ζ_1, ζ_2, τ_1, τ_2), they are satisfied also by ($1/\zeta_1$, $1/\zeta_2$, τ_1, τ_2).

In what follows, the relations $\zeta_2 = \theta$ and $\tau_2 = \phi \tau_1$ will be prescribed with θ and ϕ as given parameters. These relations and Eqs. (6) and (7)

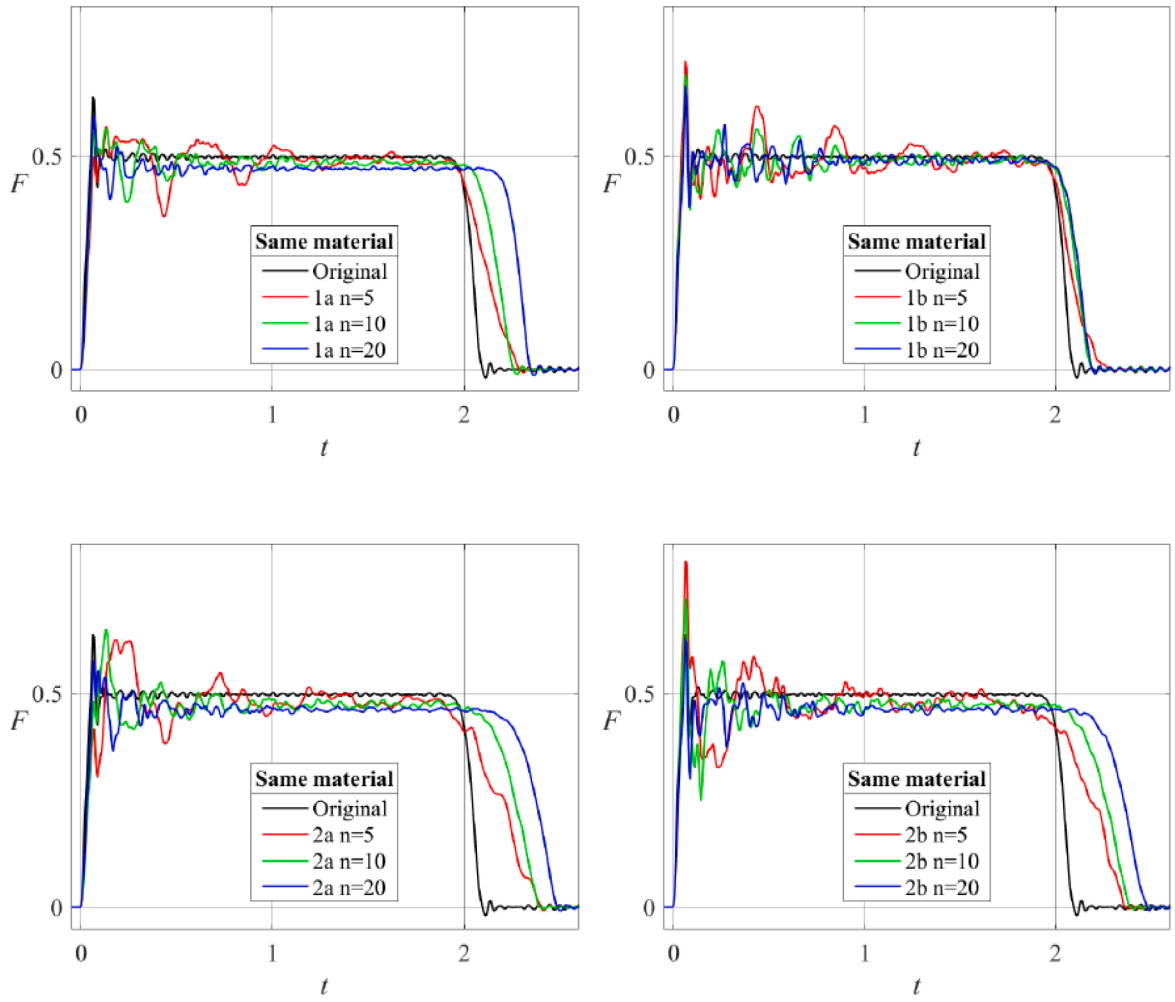

Fig. 5. Impact force histories from 3D FE simulations of original hammer and substitute hammers impacting a semi-infinite uniform rod with the same characteristic impedance as the original hammer. The substitute hammers are constituted by $n = 5$, 10 and 20 periods, and the hammers and the rod are made of the same material.

form a system of four algebraic equations with the solution

$$\zeta_1 = p + \left(p^2 + 1\right)^{1/2}, \tag{8}$$

$$\zeta_2 = \theta \tag{9}$$

$$\tau_1 = 1/(\zeta_1 + \phi\theta) \tag{10}$$

$$\tau_2 = \phi\tau_1 \tag{11}$$

where

$$p = \frac{1}{2}\phi\left(\theta^{-1} - \theta\right). \tag{12}$$

It can be shown that if the parameters (ϕ, θ) give the solution $(\zeta_1, \zeta_2, \tau_1, \tau_2)$, the parameters $(\phi, 1/\theta)$ give the solution $(1/\zeta_1, 1/\zeta_2, \tau_1, \tau_2)$. From Eq. (3), with $c_1 = c_2 = c_0$ as assumed, the hammer length ratio can be expressed as

$$\frac{L_*}{L_0} = \tau_1 + \tau_2 \tag{13}$$

which shows that the substitute hammers of this pair have the same hammer length ratio L_*/L_0. In the simulations which follow, two such pairs of substitute hammers with parameters (ϕ, θ) and $(\phi, 1/\theta)$ will be considered.

3. Simulation

3.1. Original and substitute hammers

Impact with velocity V_0 of a uniform original hammer and four of its substitute hammers oon a semi-infinite uniform rod with the same characteristic impedance Z_0 as the original hammer were simulated 1D and 3D.

The substitute hammers were defined by the number of periods n and by the dimensionless parameters (ϕ, θ) defining a period. From these parameters, given in Table 1, the dimensionless parameters $(\zeta_1, \zeta_2, \tau_1, \tau_2)$ were determined from Eqs. (8)–(12). They are shown in Table 2 together with the hammer length ratio L_*/L_0 obtained from Eq. (13).

For the 3D FE simulations, the diameter and length of the uniform original hammer were taken to be 30 mm and 800 mm, respectively, and those of the impacted uniform rod were taken to be 30 mm and 3 000 mm, respectively. With this choice, influence on the impact force by a reflected wave from the free end of the impacted rod was avoided during the time interval of interest. The elastic moduli, densities, and Poisson's ratios of the original hammer and the rod were set to be 200 GPa, 8 000 kg/m^3, and 0.3, respectively, and the impact velocity was chosen to be 10 m/s.

In a 3D context, the individual values of the cross-sectional area A, the Young's modulus E and the density ρ, together defining the characteristic impedance $Z = A(E\rho)^{1/2}$, are significant. Therefore, 3D simulations were carried out with substitute hammers of two types, viz. one

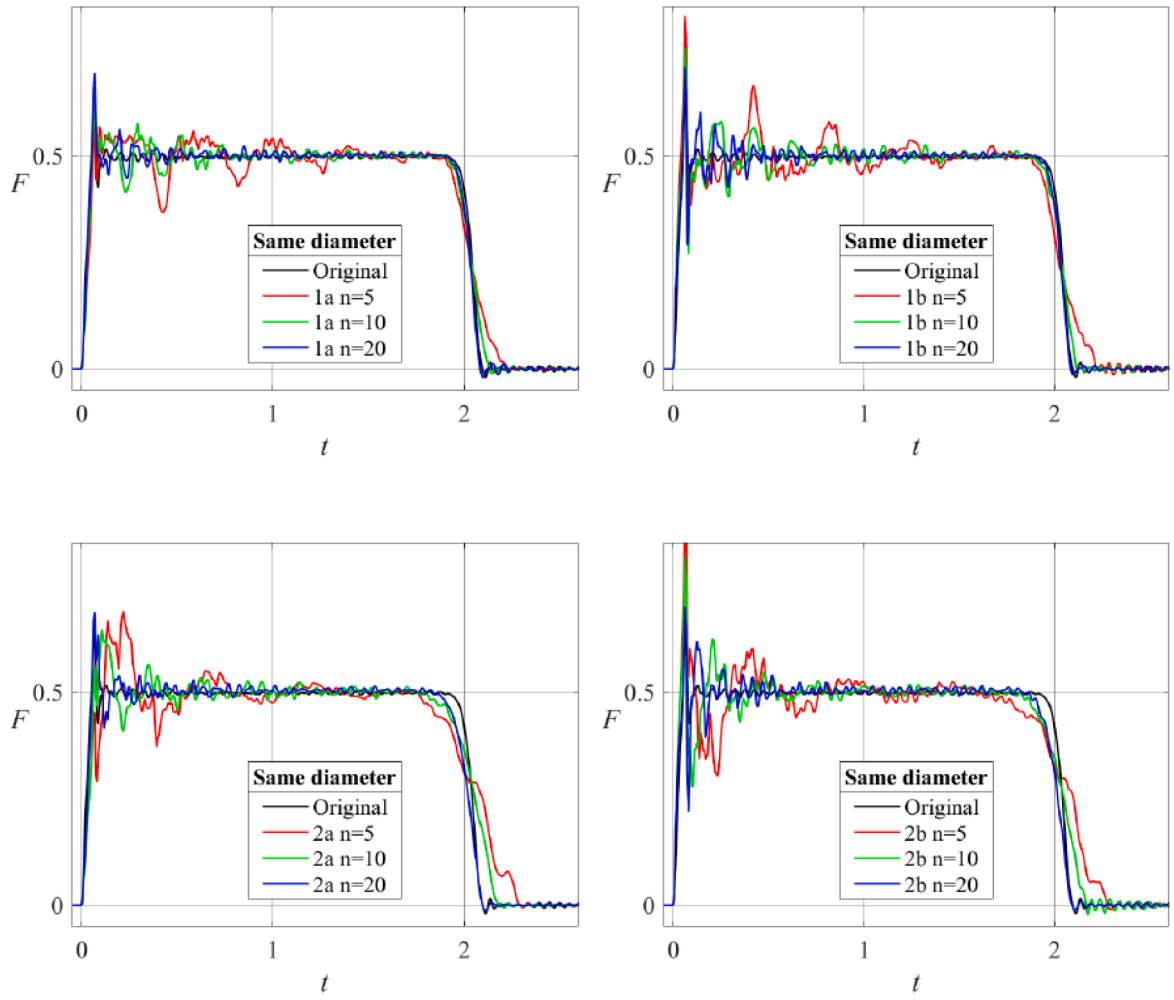

Fig. 6. Impact force histories from 3D FE simulations of original hammer and substitute hammers impacting a semi-infinite uniform rod with the same characteristic impedance as the original hammer. The substitute hammers are constituted by $n = 5$, 10 and 20 periods, and the hammers and the rod have the same diameter.

with constant material properties and variable diameter, and another with constant diameter and variable material properties. For the case of constant material properties, the diameters and lengths of the substitute hammers, obtained from their dimensionless counterparts, are shown in Table 3 together with the hammer length ratio L_*/L_0. For the case of constant diameter, the material properties and lengths were determined from the relations $E_i = \zeta_i E_0$, $\rho_i = \zeta_i \rho_0$, and $l_i = \tau_i l_0$ given that the elastic wave speeds $c_1 = c_2 = c_0$ were the same. The material properties and lengths of the constant-diameter substitutes are shown in Table 4 together with the hammer length ratio L_*/L_0.

The number of periods of the substitute hammers were chosen to be $n = 5$, 10, and 20. The substitute hammers with constant material and those with constant diameter are illustrated for $n = 10$ in Figs. 2 and 3, respectively, together with the original hammer and the impacted rod.

3.2. Impact force

The impact force F was normalized to the force $Z_0 V_0$, which is the impact force generated if the original hammer impacts a rigid stationary wall with velocity V_0, and the time t was normalized to nt_0, which is the wave transit time through the original hammer. The 1D impact force histories are shown in Fig. 4. The 3D impact force histories for the constant-material substitute hammers are shown in Fig. 5, and for the constant-diameter substitute hammers they are shown in Fig. 6.

3.3. Efficiency

The efficiency of kinetic impact energy conversion to work during the reflection of the impact-generated wave at the bit-rock interface in an idealized top hammer drill was simulated 1D for the original and substitute hammers with $n = 10$ periods shown in Fig. 2. The drill rod was assumed to be uniform and ended with a bit in contact with the rock. The bit-rock interaction was assumed to bi-linear [4,5] with penetration resistance (force per unit penetration) k during loading and k/γ during unloading with $\gamma = 0.1$. The parameter γ can be interpreted as the fraction of reversible penetration or work during primary loading.

The efficiency η as a function of the dimensionless parameter $\beta = 2kL_0/A_0E_0$, where L_0 is the length of the original hammer, is shown in Fig. 7 for the hammers in Fig. 2. Values of $\beta \ll 1$ correspond to drilling in soft rock and values $\beta \gg 1$ correspond to drilling in hard rock.

3.4. Simulation software

The 1D simulations were made with the computer program PRDS 1.5.1. The main algorithms used in this program are presented in [17]. The 3D simulations were made with the FE software LS-Dyna. In these simulations the contact between the hammer and the rod was modelled with the penalty method, and the total number of linear tetrahedral elements was around 700 000.

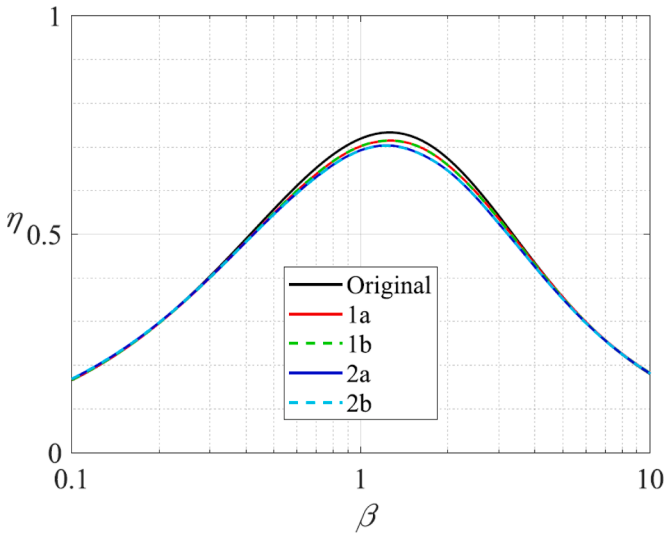

Fig. 7. Efficiency η from 1D simulation for the hammers shown in Fig. 2 based on first wave reflection at bit-rock interface versus dimensionless parameter $\beta = 2kL_0/A_0E_0$, where k is the penetration resistance, L_0 is the original hammer length, A_0 is the cross-sectional area of the original hammer and the drill rod, and E_0 is the Young's modulus. Ten percent of the work during crushing is assumed to be reversible, $\gamma = 0.1$. Comparison between original hammer and substitute hammers constituted by $n = 10$ periods.

4. Discussion

It follows from Section 2.3 that the constant characteristic impedance of a uniform original hammer can be replaced by one that is axially periodic in an infinite number of ways so that the result becomes a shorter hammer with the same mass as the original hammer. Thus, the conditions for hammer mass and hammer length can always be fulfilled. To which extent the condition for impact force history can be fulfilled is illustrated by the extent of agreement between the results of the 1D simulations shown in Fig. 4 and the 3D simulations shown in Figs. 5 and 6. This condition states that a substitute hammer should generate approximately the same impact force history as the original hammer if the impacted body is the same.

If the three conditions are fulfilled, a substitute hammer has been realized. It could replace an original uniform hammer of a percussive rock drill without effect on the impact velocity and impact frequency, which depend on the mass of the hammer, or on the efficiency of kinetic impact energy conversion to work, which depends on the impact force history. In applications with space constraints such a replacement of an original hammer with a substitute hammer could be of interest as it would allow the rock drill to be shorter. However, factors such as strength, fatigue and cost of production would have to be carefully addressed.

The method used to find substitute hammers can be applied also to an original hammer described as piecewise uniform rather than uniform. Then the mass and compliance of each uniform part of the original hammer should be redistributed the same way as done here for a uniform original hammer.

In a 1D context, there is no difference between corresponding substitute hammers shown in Figs. 2 and 3. The wave phenomena are controlled by the characteristic impedance $Z = A(E\rho)^{1/2}$ of each cross section, which is the same in corresponding substitute hammers. The individual values of the cross-sectional area A, the Young's modulus E and the density ρ are insignificant as long as the product $A(E\rho)^{1/2}$ is the same. The 1D impact force histories generated by these pairs of hammers (1a, 1b; 2a, 2b) with $n = 5$, 10 and 20 periods are shown in Fig. 4. They all agree well with that generated by the original hammer. Thus, the force amplitudes are oscillating around 0.5, and the durations at half the average amplitude are close to 2 in agreement with the exact 1D results for the original hammer.

If the hammers shown in Figs. 2 and 3 could serve as substitute hammers also in a 3D context depends on the extent to which the condition c) for impact force history is fulfilled, which can be judged from the results of simulations shown in Figs. 5 and 6, respectively. For the case of constant material and variable diameter, Fig. 5 shows that, besides from oscillations similar to those in Fig. 4, the impact force pulses have approximately rectangular shape. However, the hammers generate somewhat lower amplitudes and longer durations than the original hammer. Also, the amplitude of the pulse decreases and its length increases with increasing number of hammer periods. The best agreement with the original hammer is obtained for the lowest number of periods $n = 5$ and for the substitute hammer 1b. For the case of constant diameter and variable material, Fig. 6 shows results for the impact force pulse that are close to the 1D results in Fig. 4, both locally and globally. Thus, hammers of the types shown in Fig. 2 with constant material and variable diameter may give rise to significant 3D effects while those with constant diameter and variable material shown in Fig. 3 give rise to much smaller 3D effects. Yet, the former types of hammers may serve as substitute hammers when 3D effects are small enough.

The reason for the lower amplitudes and longer durations of the force pulses with variable diameter than with constant diameter is that initially plane cross-sections with abrupt changes of diameter do not remain plane as assumed in 1D theory. Instead, the material on the smaller-diameter side of the abrupt change "indents" the material on the larger-diameter side, and the effect of "indentation" increases with increasing ratio of larger to smaller diameter. Therefore, each cross section of a hammer period with abrupt change of diameter increases the compliance of the period compared to the value predicted by 1D theory. As a result, the compliance of the hammer increases with increased number of hammer periods. Increased compliance results in a softer impact which in turn decreases the amplitude and increases the duration of the impact force pulse.

In the examples shown here, a substitute hammer period has been defined by two characteristic impedances and two lengths as shown in Fig. 1. However, a period can be defined by a number of characteristic impedances and lengths larger than two. In this way, the jumps in characteristic impedance can be made smaller which is expected to reduce the 3D effect of "indentation".

For the efficiency obtained by use of the original hammer, the exact 1D result is $\eta = 2(1-\gamma)(1-e^{-\beta})^2/\beta$ [4] which agrees closely with the results of simulation shown in Fig. 7. For $\beta = 1.26$ and $\gamma = 0.1$ the maximum efficiency is 0.734. Soft and hard conditions correspond to $\beta \ll 1$ and $\beta \gg 1$, respectively. Generally, the substitute hammers studied give slightly lower efficiencies than the original hammer. The largest difference is obtained under drilling in medium hard rock with $\beta \sim 1$, where it is a few percent. From an application point of view, this difference due to the oscillations shown in Fig. 4 is negligible.

5. Conclusion

A method has been developed for realization of short substitutes for an original hammer of a percussive rock drill which may be of interest in applications with space constraints. For an original hammer described as uniform, examples have been shown of substitute hammers with axially periodic characteristic impedance having the same mass as the original hammer, being shorter than the original hammer, and generating approximately the same impact force history as the original hammer. Because of the mentioned properties of substitute hammers, any such hammer can replace the original hammer and allow shorter rock drills without significantly changing the impact energy, impact frequency and efficiency of the rock drill. The method works well as long as 3D effects are small enough. It can be applied also to an original hammer described as piecewise uniform. Then the mass and compliance of each uniform part of the original hammer should be redistributed the same way as for

a uniform original hammer.

CRediT authorship contribution statement

J. Huo: Methodology, Validation, Formal analysis, Investigation, Writing – review & editing. **B. Lundberg:** Conceptualization, Methodology, Formal analysis, Investigation, Writing – review & editing.

Declaration of Competing Interest

The authors declare that they have no known competing financial interests or personal relationships that could have appeared to influence the work reported in this paper.

Data availability

No data was used for the research described in the article.

References

[1] Fairhurst C. Wave mechanics of percussive drilling. Mine Quarry Eng 1961;27:122–30. 169-78, 327-8.
[2] Simon R. Transfer of the stress wave energy of a percussive drill to the rock. Int J Rock Mech Min 1964;1(3):397–411. https://doi.org/10.1016/0148-9062(64)90006-3.
[3] Hustrulid WA, Fairhurst C. A theoretical and experimental study of the percussive drilling of rock part II – force-penetration and specific energy determinations. Int J Rock Mech Min 1971;8(4):335–56. https://doi.org/10.1016/0148-9062(71)90046-5.
[4] Lundberg B. Energy transfer in percussive rock I: comparison of percussive methods. Int J Rock Mech Min 1973;10(5):381–99. https://doi.org/10.1016/0148-9062(73)90024-7.
[5] Lundberg B, Huo J. Biconvex versus bilinear force-penetration relationship in percussive drilling of rock. Int J Impact Eng 2017;100:7–12. https://doi.org/10.1016/j.ijimpeng.2016.10.002.
[6] Long VF. An investigation aimed at improving the efficiency of percussive rock drilling. J S Afr I Min Metall 1966;66:276–96.
[7] Lundberg B, Collet P. Optimal wave with respect to efficiency in percussive drilling with integral drill steel. Int J Impact Eng 2010;37(8):901–6. https://doi.org/10.1016/j.ijimpeng.2010.02.001.
[8] Goldsmith W. Impact: the theory and physical behaviour of colliding solids. 1st ed. London: Edward Arnold Publishers Ltd; 1960.
[9] Dutta PK. The determination of stress waveforms produced by percussive drill pistons of various geometrical designs. Int J Rock Mech Min 1968;5(6):501–10. https://doi.org/10.1016/0148-9062(68)90038-7.
[10] Luciano CE, Dante AE. A 3D FEM methodology for simulating the impact in rock-drilling hammers. Int J Rock Mech Min 2008;45(5):701–11. https://doi.org/10.1016/j.ijrmms.2007.08.001.
[11] Lundberg B, Lesser M. On impactor synthesis. J Sound Vib 1978;58(1):5–14. https://doi.org/10.1016/S0022-460X(78)80056-X.
[12] Zhu P, Liu DS, Peng YD, Chen AH. Inverse approach to determine piston profile from impact stress waveform on given non-uniform rod. Trans Nonferrous Met Soc 2001;11(2):297–300.
[13] Burgert J. On direct and inverse problems related to longitudinal impact of non-uniform elastic rods [dissertation]. Karlsruhe: Karlsruhe Institute of Technology; 2020. https://doi.org/10.5445/KSP/1000129237.
[14] Burgert J, Seemann W, Lundberg B. Recursive algorithm for the distribution of characteristic impedance of an elastic rod producing a prescribed impact force history on a given elastic rod. Int J Impact Eng 2022;161:104133. https://doi.org/10.1016/j.ijimpeng.2021.104133.
[15] Nygren T. Transmission of waves through elastic and viscoelastic junctions [dissertation]. Uppsala: Uppsala University; 1998.
[16] Nygren T, Andersson LE, Lundberg B. Synthesis of elastic junctions with wave transmission properties of a given junction. Wave Motion 1999;30(2):143–58. https://doi.org/10.1016/S0165-2125(99)00002-5.
[17] Lundberg B. Microcomputer simulation of stress wave energy transfer to rock in percussive drilling. Int J Rock Mech Min 1982;19(5):229–39. https://doi.org/10.1016/0148-9062(82)90221-2.